

## A Theoretical Study of Pyrolysis Mechanisms of Pyrrole

Lei Zhai, Xuefeng Zhou, and Ruifeng Liu\*

Department of Chemistry, East Tennessee State University, Johnson City, Tennessee 37614

Received: October 26, 1998; In Final Form: February 26, 1999

Density functional theory and ab initio calculations were carried out to investigate the pyrolysis mechanisms of pyrrole. All equilibrium and transition state structures of the proposed reaction channels were fully optimized by the density functional B3LYP method using the 6-31G(d,p) basis set. Relative energies were evaluated at the QCISD(T)/6-311G(d,p) level of theory. In addition to the mechanism proposed in experimental studies, alternative unimolecular pathways for the formation of *cis*-crotonitrile and allyl cyanide, major nitrogen-containing isomerization products, were proposed and investigated. The results suggest that a mechanism proposed in the present study is more likely responsible for the formation of allyl cyanide. For the formation of *cis*-crotonitrile, a mechanism proposed in the present study should also be competitive, especially under low-pressure conditions. Although extensive calculations were carried out, we failed to identify a unimolecular decomposition pathway generating HCN, another major nitrogen-containing pyrolysis product, with an activation barrier close to the experimental value.

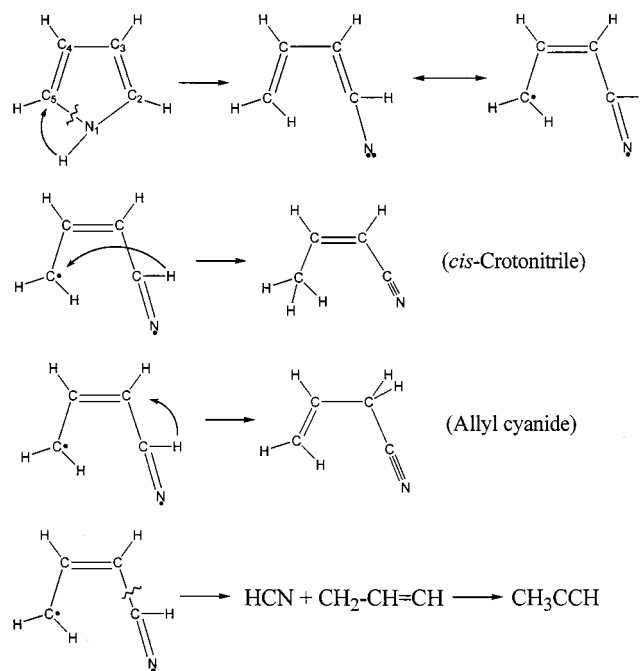
### Introduction

Heavy fuels such as coal and coal-derived liquids consist of a complex mixture of aromatic hydrocarbons and heterocyclic aromatic compounds containing nitrogen, oxygen, and sulfur.<sup>1,2</sup> The combustion of these fuels, used as an energy source in many power plants, results in the formation of many nitrogen oxides (NO<sub>x</sub>),<sup>3–7</sup> which contribute to such environmental hazards as acid rain and smog. Many methods have been proposed to reduce NO<sub>x</sub> formation. Those that showed promise include methods of thermal deNO<sub>x</sub><sup>8</sup> or RAPRENO<sub>x</sub><sup>9</sup> and combustion modification techniques such as NO reburning. However, none of the methods is completely satisfactory, partly due to the fact that the complete combustion mechanism of heavy fuels is still unknown.

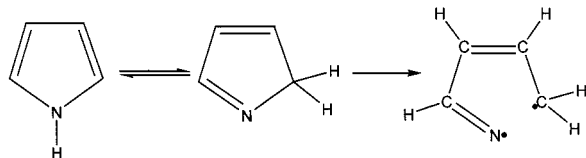
It is well-known that chemically bound nitrogen in coal and coal-derived liquids is predominantly in the form of heterocycles such as pyrrole and pyridine ring systems.<sup>1,2,10–12</sup> Under combustion conditions these heterocycles may form nitrogen precursors of NO<sub>x</sub>, and the rate of precursor formation may determine the rate of NO<sub>x</sub> formation. Thus, it is important to understand the reaction mechanism and kinetics of these heterocycles at combustion temperatures. Contrary to the wide spread use of these fuels, there have been only a few detailed studies of pyrolysis reactions of pyrrole and pyridine rings. To date, the most comprehensive studies were carried out by Lifshitz et al.<sup>13–16</sup> and by Mackie et al.<sup>17,18</sup> They identified<sup>13,17</sup> that the major products of pyrrole pyrolysis over the temperature range 1050–1700 K are *cis*-crotonitrile (CH<sub>3</sub>CH=CHCN), HCN + C<sub>3</sub>H<sub>4</sub> (propyne and allene), and allyl cyanide (CH<sub>2</sub>=CHCH<sub>2</sub>CN) with a branching ratio of approximately 3.5:1.5:1. Lifshitz et al. proposed<sup>13</sup> that these products were formed via a common open-chain biradical intermediate, as described in Scheme 1.

The initial step of this mechanism is a concerted N<sub>1</sub>–C<sub>5</sub> bond cleavage and 1,2-hydrogen migration from the nitrogen to C<sub>5</sub>. The biradical thus formed can have a 1,4-hydrogen migration from C<sub>2</sub> to C<sub>5</sub> to yield *cis*-crotonitrile. The biradical can also have a 1,2-hydrogen migration from C<sub>2</sub> to C<sub>3</sub>, leading to allyl cyanide, or a C<sub>2</sub>–C<sub>3</sub> bond cleavage to form HCN and CH<sub>2</sub>–CH=CH. The latter can rearrange to yield propyne and allene.

**SCHEME 1. Pyrolysis Mechanism of Pyrrole Proposed by Lifshitz et al.<sup>13</sup>**



Mackie et al. agreed<sup>17</sup> with Lifshitz et al. on the proposal that the major products were formed via the same biradical intermediate, but they argued that a direct C–N bond cleavage is unfavorable because the C–N bond is pretty strong due to the aromatic nature of the pyrrole ring. They estimated a C–N bond dissociation energy of 90 kcal/mol, which is significantly higher than the activation energy of 74–75 kcal/mol for overall disappearance of pyrrole derived from rate constants. The difference suggests that the observed barrier may not correspond to a direct ring scission. They proposed that the first step of pyrrole pyrolysis is a 1,2-hydrogen migration from nitrogen to C<sub>2</sub> to form 2*H*-pyrrole (pyrrolene), followed by C–N bond cleavage to yield the biradical intermediate, as described in Scheme 2.

**SCHEME 2. Mechanism of Biradical Intermediate Formation Proposed by Mackie et al.<sup>17</sup>**


Although the two groups have different opinions on the details of the biradical formation, both of them consider the biradical as an important intermediate for the formation of the observed major products. In our opinion, however, the biradical seems unlikely to play such an important role under the experimental conditions. It is known<sup>19</sup> that the bond energy of a regular C–N single bond is about 70 kcal/mol. Therefore, the barrier for the biradical formation from 2*H*-pyrrole should be around 70 kcal/mol. The biradical will be resonance stabilized. In the case of furan decomposition, a resonance stabilization energy of 7 kcal/mol was suggested.<sup>20,21</sup> Taking into account resonance stabilization of a similar magnitude, one would reasonably expect the biradical intermediate to be about 60 kcal/mol higher in energy than 2*H*-pyrrole. As 2*H*-pyrrole does not preserve aromaticity, it should be higher in energy than pyrrole. Thus one can safely assume that if the biradical intermediate exists, it should be at least 60 kcal/mol higher in energy than pyrrole. According to Lifshitz et al., to form HCN from the biradical the C–C(H)N bond, which has a bond order between 1 and 2 due to  $\pi$  conjugation, should be ruptured. The bond energy of a regular C–C single bond is over 80 kcal/mol.<sup>19</sup> If half of the bond energy is required to break the CC bond, the transition state would be over 100 kcal/mol higher than pyrrole. The experimental<sup>13</sup> activation energies for HCN and C<sub>3</sub>H<sub>4</sub> (propyne and allene) formation are 84 and 73 kcal/mol, respectively. They are significantly lower than the expected energy barrier from bond energy considerations. Along a similar line of consideration, one would also expect that formation of *cis*-crotonitrile via the biradical intermediate requires a higher activation energy than the experimental value of 72 kcal/mol.<sup>13</sup> These considerations indicate that if the observed products were formed via an intermediate, the intermediate must be more stable than the biradical so that excess energy is available for subsequent bond cleavage, or the activation energies for the product formation must be higher than the reported values. To understand the details of major nitrogen-containing product formation under pyrolytic conditions, we carried out a detailed theoretical investigation of isomerization and decomposition channels of pyrrole. The results are reported herein.

**Computational Details**

All equilibrium and transition state structures along the proposed unimolecular isomerization and decomposition pathways were fully optimized by Becke's three-parameter hybrid density functional theory–Hartree–Fock method<sup>22</sup> using Lee–Yang–Parr's correlation functional<sup>23</sup> (B3LYP) and the 6-31G(d,p) basis set.<sup>24</sup> Vibrational analyses were carried out at the same level of theory on the optimized structures to characterize them as either equilibrium structures (all real harmonic vibrational frequencies) or transition states (one and only one imaginary vibrational mode corresponding to the reaction coordinate). Intrinsic reaction coordinate (IRC) calculations were carried out on most of the transition structures to confirm that they lead to the desired reactants and products. Zero point vibrational energies (ZPE) were taken into account and were

approximated by one-half of the sum of B3LYP/6-31G(d,p) harmonic vibrational frequencies. To obtain more reliable estimates of activation energies for the reaction channels, single point energy calculations were performed on B3LYP/6-31(d,p) structures using the quadratic configuration interaction method with single, double, and perturbative triple substitutions (QCISD(T)). A larger 6-311G(d,p) basis set was used for the single point energy calculations. For the open-shell singlet species (the biradical intermediate and related open-shell transition states), the unrestricted Hartree–Fock like B3LYP method (uB3LYP) was used for geometry optimizations, and unrestricted QCISD(T) (uQCISD(T)) was used to evaluate relative energies. All the calculations were performed using the Gaussian94 program package.<sup>25</sup>

**Results and Discussion**

We first investigated the biradical formation processes proposed in the two experimental studies.<sup>13,17</sup> Our extensive calculations failed to locate a transition state for concerted C–N bond cleavage and hydrogen migration from the nitrogen to a neighboring carbon, the first step of the pyrolysis mechanism proposed by Lifshitz et al. (Scheme 1). Geometry optimization for the transition state by B3LYP/6-31G\*\* easily leads to a transition state for hydrogen migration from nitrogen to an adjacent carbon, yielding 2*H*-pyrrole. Thus the calculations seem to support the proposal of Mackie et al. for the initial step of pyrrole pyrolysis (Scheme 2).

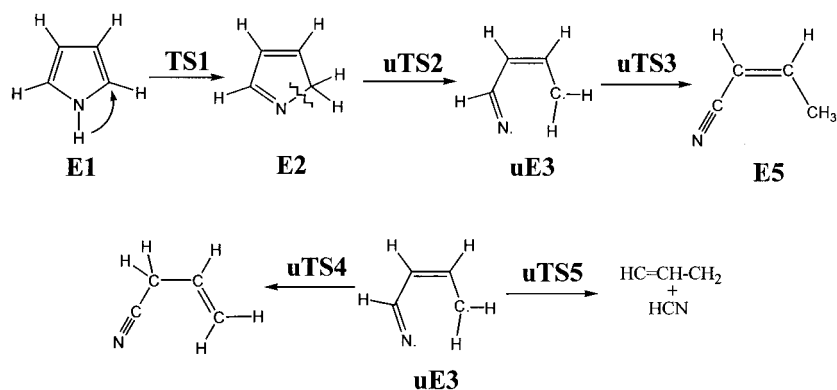
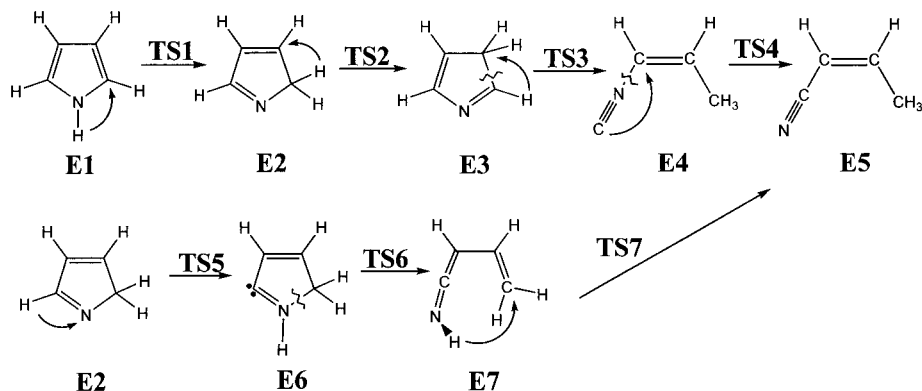
According to both Lifshitz et al. and Mackie et al., the main pyrolysis channels proceed via an open-chain biradical intermediate. We therefore investigated the ring-opening reaction of 2*H*-pyrrole and subsequent isomerization and decomposition processes of the open-shell biradical by uB3LYP. These processes are described in Scheme 3. In this scheme, **uE3**, **uTS2**, **uTS3**, **uTS4**, and **uTS5** represent open-shell singlet equilibrium and transition state structures. In addition, we also investigated two additional channels leading to the formation of *cis*-crotonitrile, the most prominent nitrogen-containing isomerization product, with B3LYP in the closed-shell singlet domain. These channels are described in Scheme 4.

These two channels look more complicated than the mechanism proposed by Lifshitz et al. and Mackie et al., but the intermediates involved are expected to be relatively stable and low in energy. Thus, even though more reaction steps are involved along these channels, the intermediates may carry sufficient energy for subsequent reaction steps.

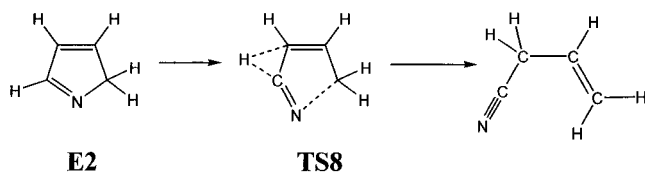
We also investigated the formation of allyl cyanide from 2*H*-pyrrole via a concerted transition state of C–N bond cleavage and hydrogen migration, as described in Scheme 5, and the formation of HCN and C<sub>3</sub>H<sub>4</sub> from 2*H*-pyrrole via a concerted transition state for C–N and C–C bond cleavages as described in Scheme 6. Both Schemes 5 and 6 are in the closed-shell singlet domain and therefore investigated by B3LYP.

Prominent structural features of the equilibrium and transition state structures along the proposed reaction pathways optimized by B3LYP/6-31G(d,p) and uB3LYP/6-31G(d,p) are presented schematically in Figure 1. In this figure, bond distances are given in Ångstroms and angles in degrees. For pyrrole, experimental structural parameters derived from microwave spectra<sup>26</sup> are also given in this figure for comparison. As we can see, the calculated and experimental structural parameters are in good agreement, the largest deviation between the calculated and microwave bond angles is 0.3°, and the deviation between the calculated and experimental bond lengths is smaller than 0.01 Å.

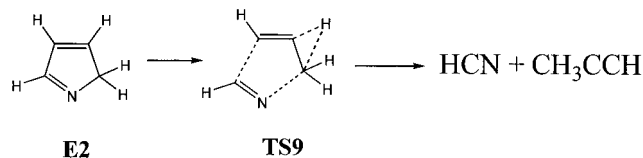
Energies of the optimized structures evaluated at uB3LYP/6-31G(d,p), uQCISD/6-311G(d,p), and uQCISD(T)/6-311G(d,p)

SCHEME 3. Pyrolysis Mechanism of Pyrrole Proposed by Lifshitz et al.<sup>13</sup> with Slight Modification by Mackie et al.<sup>17</sup>SCHEME 4. Isomerization Mechanism Leading to the Formation of *cis*-Crotonitrile Proposed in the Present Study

SCHEME 5. Isomerization Mechanism Leading to the Formation of Allyl Cyanide Proposed in the Present Study



SCHEME 6. Decomposition Mechanism Leading to the Formation of HCN and Propyne Investigated in the Present Study



levels of theory are presented in Table 1. In this table, the energy of pyrrole is given in Hartrees. The energies of all other structures are given in kcal/mol relative to that of pyrrole. Schematic energy profiles of the reaction pathways yielding *cis*-crotonitrile and allyl cyanide are presented in Figures 2 and 3. The results support the conclusion of Mackie et al.<sup>17</sup> that 1,2-hydrogen migration in pyrrole to yield *2H*-pyrrole is a facile process. At the QCISD(T)/6-311G(d,p) level of theory and with ZPE correction, the activation barrier is predicted to be 44 kcal/mol. The product, *2H*-pyrrole, is predicted to be 10.6 kcal/mol higher in energy than pyrrole, which is in line with expectation. The heavy atom skeleton of the transition state, TS1, is nearly planar while the migrating hydrogen is out of plane of the heavy

atom skeleton. The product, E2 (*2H*-pyrrole), is predicted to have *C<sub>s</sub>* symmetry with normal single and double bond lengths.

In line with expectation, the transition state for the biradical formation, uTS2, is 72.9 kcal/mol higher than pyrrole at the highest level of theory, and the biradical, uE3, is resonance stabilized by 6.5 kcal/mol compared to the transition state uTS2. According to Lifshitz et al. (Scheme 3), starting from the biradical intermediate, a 1,4-hydrogen migration leads to *cis*-crotonitrile. The transition state, uTS3, optimized by uB3LYP/6-31G(d,p) was found to be 81.8 kcal/mol higher than pyrrole. This is significantly higher than the experimental activation energy of CH<sub>3</sub>CH=CHCN (both *cis* and *trans*) formation, 72 kcal/mol.<sup>13</sup> IRC calculation indicates that uTS3 leads to *cis*-crotonitrile, but not uE3. Instead, it leads to a planar rotational isomer around the CH–C(H)N bond. In this isomer, the hydrogen is pointing toward the carbon it migrates to. In a recent study,<sup>27</sup> Dubnikova and Lifshitz showed that this isomer is less than 1 kcal/mol higher in energy than uE3, and the transition state connecting the two isomers is about 70 kcal/mol higher than pyrrole.

Starting from the biradical intermediate, a 1,2-hydrogen migration via transition state uTS4 leads to the formation allyl cyanide. However, the calculated activation barrier, 88.3 kcal/mol, is much higher than the reported experimental value, 77 kcal/mol. According to Lifshitz et al., a C–C bond cleavage in the biradical yields HCN and C<sub>3</sub>H<sub>4</sub> (propyne and allene). The calculations indicate that the transition state of C–C bond cleavage, uTS5, is 110.3 kcal/mol higher than pyrrole. It is in line with our expectation, but much higher than the experimental activation energy, 84 kcal/mol of HCN formation,<sup>13</sup> and 73 kcal/mol of propyne and allene formation.<sup>13</sup>

Following Scheme 4, the results in Table 1 indicate that other than a C–N bond cleavage, *2H*-pyrrole can easily isomerize

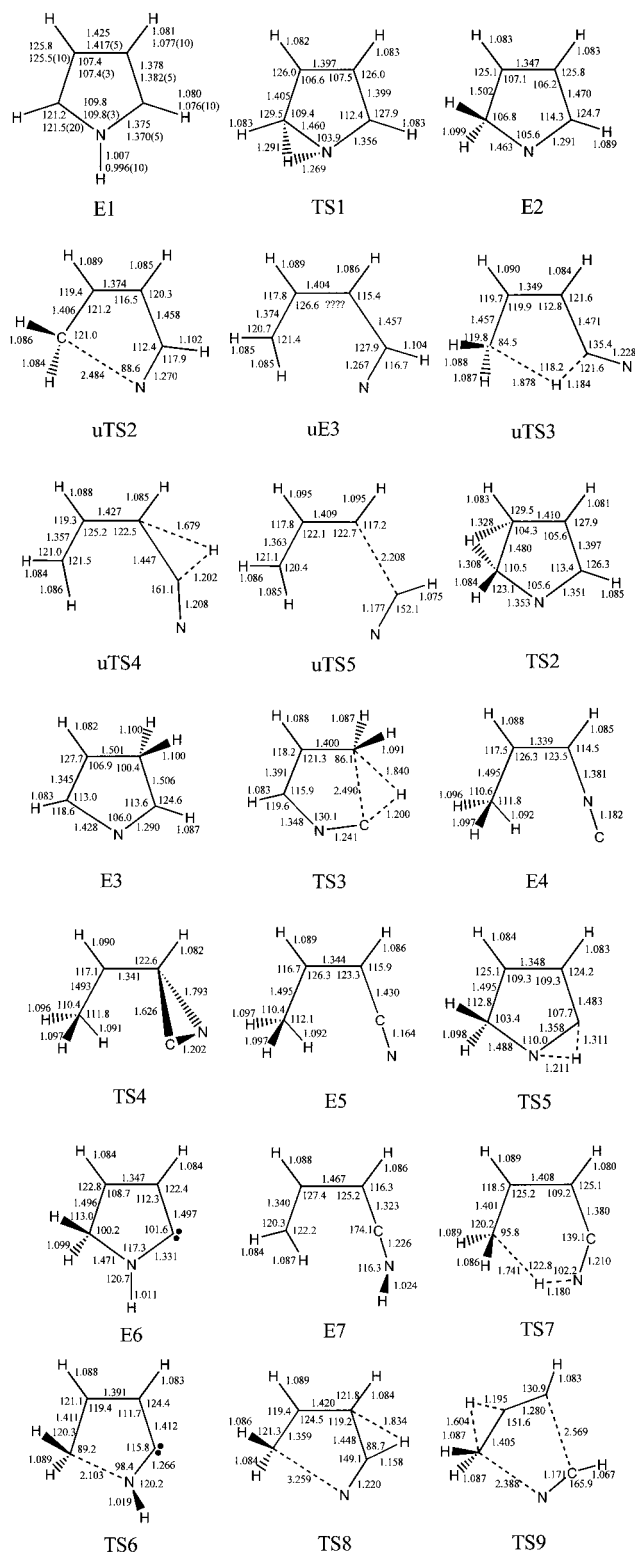


**Figure 1.** uB3LYP/6-31G(d,p) structural parameters of the critical structures along the proposed pyrolysis mechanisms of pyrrole (Schemes 3–6). Bond lengths are given in Ångströms, and angles, in degrees. For **E1** (pyrrole) the first entry is the B3LYP/6-31G(d,p) result and the second entry is the microwave structural parameter (from ref 26) with uncertainty given in parentheses.

via another 1,2-hydrogen migration to yield *3H*-pyrrole. The transition state of this hydrogen migration, **TS2**, is only 38.8 kcal/mol higher than pyrrole. *3H*-Pyrrole is predicted to be 1.5 kcal/mol higher in energy than *2H*-pyrrole. *3H*-Pyrrole can rearrange to *cis*-isocyanocrotonitrile (**E4**) via a concerted transition state (**TS3**) of C<sub>2</sub>–C<sub>3</sub> bond cleavage and 1,2-hydrogen

**TABLE 1: Energies<sup>a</sup> of the Equilibrium and Transition Structures<sup>b</sup> along the Proposed Reaction Channels<sup>c</sup> of Pyrrole Pyrolysis**

structure <sup>b,c</sup>	B3LYP <sup>d</sup>		uQCISD	uQCISD(T)	$\Delta E^{\ddagger}$
	<i>E</i> <sup>a</sup>	ZPE <sup>e</sup>	6-311G(d,p)	6-311G(d,p)	
<b>E1</b>	-210.17634	51.9	-209.62059	-209.65477	0.0
<b>TS1</b>	47.1	48.7	49.1	47.1	43.9
<b>E2</b>	13.8	51.1	11.3	11.4	10.6
<b>uTS2</b>	74.1	47.5	76.0	77.3	72.9
<b>uE3</b>	68.5	47.5	68.8	71.6	67.2
<b>uTS3</b>	85.1	45.2	88.0	88.5	81.8
<b>uTS4</b>	90.6	45.3	93.9	94.9	88.3
<b>uTS5</b>	118.8	46.1	118.0	116.1	110.3
<b>TS2</b>	41.3	49.0	43.1	41.8	38.8
<b>E3</b>	16.1	50.8	13.1	13.2	12.1
<b>TS3</b>	85.1	46.8	89.9	85.5	80.4
<b>E4</b>	31.5	49.4	25.7	26.9	24.4
<b>TS4</b>	69.3	47.8	64.2	63.6	59.4
<b>E5</b>	9.4	49.8	3.7	4.4	2.3
<b>TS5</b>	94.2	47.3	92.2	91.0	86.4
<b>E6</b>	51.3	51.0	45.8	46.9	46.0
<b>TS6</b>	79.1	49.0	81.9	77.3	74.3
<b>E7</b>	35.8	46.7	36.4	36.6	33.7
<b>TS7</b>	73.1	49.8	76.4	72.1	66.9
<b>TS8</b>	94.4	46.3	95.5	89.2	83.6
<b>TS9</b>	134.3	42.7	129.6	125.7	116.5
allyl cyanide	16.0	49.7	7.5	8.7	6.5
HCN + propyne	57.9	45.2	45.0	46.4	39.7

<sup>a</sup> The total energy of pyrrole (**E1**) is given in Hartrees; the energies of other structures are given in kcal/mol relative to **E1**. <sup>b</sup> The structures were optimized by B3LYP/6-31G(d,p); they are given in Figure 1. <sup>c</sup> The proposed reaction channels are described in Schemes 3–6. <sup>d</sup> The 6-31G(d,p) basis set was used in all B3LYP calculations. <sup>e</sup> Zero point vibrational energy in kcal/mol approximated by one-half of the sum of B3LYP/6-31G(d,p) harmonic frequencies.  $\Delta E^{\ddagger} = \Delta E(\text{uQCISD(T)}) + \Delta(\text{ZPE})$ .

migration from C<sub>2</sub> to C<sub>3</sub>. *cis*-Isocyanocrotonitrile is predicted to be 24.4 kcal/mol higher in energy than pyrrole, and it isomerizes to yield *cis*-crotonitrile with an activation barrier of 35 kcal/mol. Along this pathway, the highest energy barrier occurs at transition state **TS3** (concerted C<sub>2</sub>–C<sub>3</sub> bond cleavage and 1,2-hydrogen migration), which is 80.4 kcal/mol higher in energy than pyrrole at QCISD(T)/6-311G(d,p) plus ZPE level of theory.

The other alternative pathway of *cis*-crotonitrile formation described in Scheme 4 starts with a 1,2-hydrogen migration from carbon to nitrogen with an activation barrier of 86.4 kcal/mol at **TS5**, generating a closed-shell intermediate **E6**, which is 46 kcal/mol higher in energy than pyrrole. The C–N bond in **E6** breaks with an activation energy of 74.3 kcal/mol above pyrrole to form intermediate **E7**, which is 33.7 kcal/mol higher than pyrrole. A hydrogen migration from the nitrogen to C<sub>5</sub> in **E7** produces *cis*-crotonitrile. The highest activation barrier along this pathway occurs at **TS5** (1,2-hydrogen migration from carbon to nitrogen), which is 86.4 kcal/mol higher than pyrrole.

Schematic energy profiles of *cis*-crotonitrile formation along the three reaction channels described in Schemes 3 and 4 are presented in Figure 2. They show that the highest activation barrier of the mechanism proposed by Lifshitz et al. (81.8 kcal/mol) is very close to the highest barrier along the favorable mechanism we propose (80.4 kcal/mol). However, starting from *2H*-pyrrole Lifshitz's mechanism goes through a high-energy biradical intermediate while our mechanism proceeds via two low-energy closed-shell intermediates, *3H*-pyrrole (**E3**) and *cis*-isocyanocrotonitrile (**E7**). Thus, under low-pressure conditions, the two mechanisms may compete with each other, but under high-pressure conditions, the mechanism of Lifshitz et al. may be favorable because collisional deactivation may trap the stable intermediates along the pathway we propose.

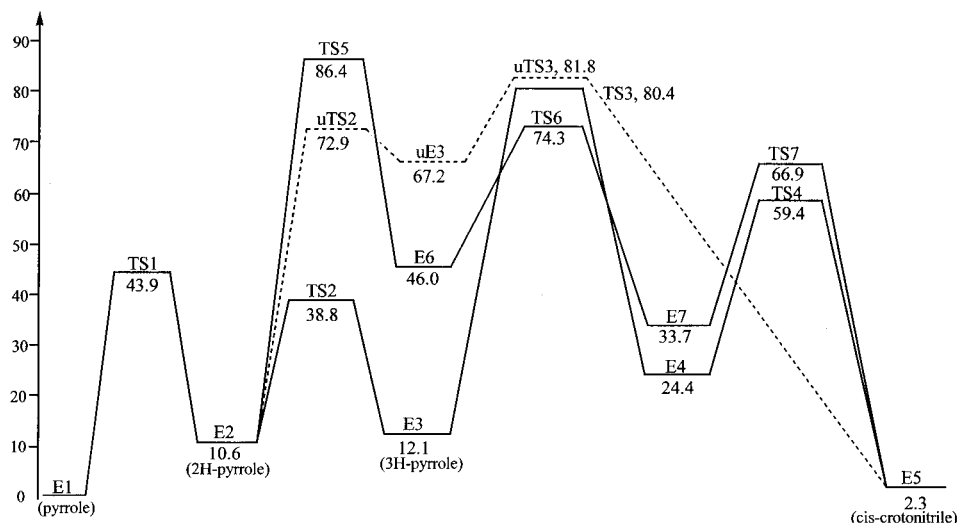


**Figure 2.** Schematic energy profiles of the formation of *cis*-crotonitrile along the proposed reaction channels described in Schemes 3 and 4. The numerical values are uQCISD(T)/6-311G(d,p) + ZPE energies in kcal/mol relative to that of pyrrole.

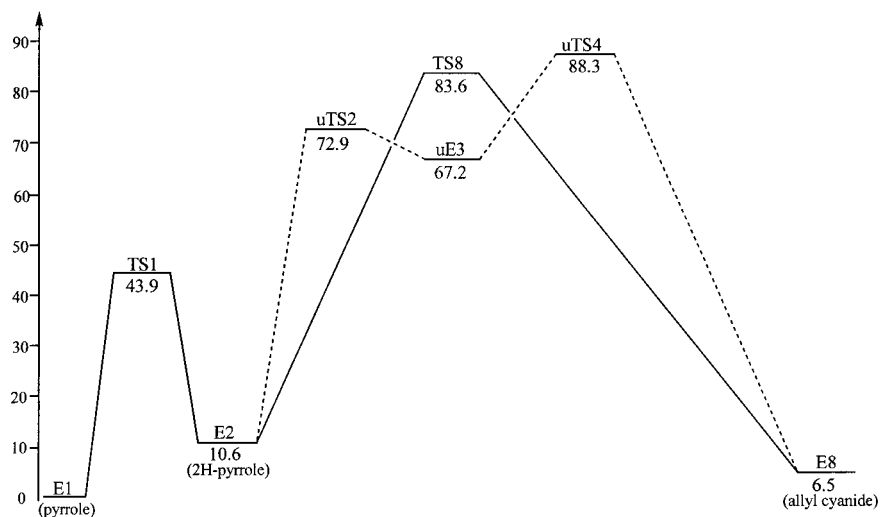


**Figure 3.** Schematic energy profiles of the formation of allyl cyanide along the proposed reaction channels described in Schemes 3 and 5. The numerical values are uQCISD(T)/6-311G(d,p) + ZPE energies in kcal/mol relative to that of pyrrole.

According to the mechanism of Lifshitz et al. (Scheme 3), allyl cyanide is formed via a 1,2-hydrogen migration from the biradical intermediate. The transition state, **uTS4**, is predicted by uQCISD(T)/6-311G(d,p) + ZPE to be 88.3 kcal/mol higher than pyrrole. The alternative mechanism of allyl cyanide formation (Scheme 5) proposed in the present study starts with 2*H*-pyrrole and proceeds through a concerted transition state of C–N bond cleavage and 1,2-hydrogen migration. The transition state (**TS8**) is predicted by QCISD(T)/6-311G(d,p) + ZPE to be 83.6 kcal/mol higher than pyrrole. Thus, allyl cyanide is more likely formed via the reaction pathway proposed in the present study. Schematic energy profiles of allyl cyanide formation are presented in Figure 3.

According to the mechanism of Lifshitz et al. (Scheme 3), HCN is also formed via the biradical intermediate by cleaving a C–C bond. They derived an activation energy of 84 kcal/mol from kinetics measurements. The transition state, **uTS5**, was located by uB3LYP/6-31G(d,p) and presented in Figure 1. However, it is predicted by uQCISD(T)/6-311G(d,p) + ZPE to be 110.3 kcal/mol higher than pyrrole. This is much higher than the experimental activation energy, but in line with our expectation from bond dissociation energy considerations. Another possible pathway of HCN formation starts with 2*H*-

pyrrole and proceeds via a concerted C–C and C–N bond cleavage and hydrogen migration, as described in Scheme 6. The transition state, **TS9**, optimized by B3LYP/6-31G(d,p) is also presented in Figure 1. It is predicted by QCISD(T)/6-311G(d,p) + ZPE to be 116 kcal/mol higher than pyrrole. Both **uTS5** and **TS9** are much higher than the experimental activation energy of 84 kcal/mol, indicating HCN must be produced via some other reaction channels. We have performed extensive calculations in an effort to find a reasonable unimolecular decomposition pathway generating HCN with an activation energy close to the experimental value. However, all plausible pathways we have investigated were predicted to have activation barriers over 100 kcal/mol. More efforts are needed to understand the details of HCN formation.

### Concluding Remarks

Density functional theory and ab initio quantum mechanical calculations were carried out to investigate the pyrolysis mechanisms of pyrrole. All equilibrium and transition state structures along the proposed reaction pathways were fully optimized by uB3LYP/6-31G(d,p), and relative energies were evaluated by uQCISD(T)/6-311G(d,p) at B3LYP/6-31G(d,p)

structures. The results support the proposal that the initial step of pyrrole pyrolysis is a 1,2-hydrogen migration to form an intermediate, 2*H*-pyrrole. Subsequent C–N cleavage results in the formation of an open-shell biradical intermediate proposed in the experimental studies. Transition states for the formation of *cis*-crotonitrile, allyl cyanide, and HCN from the biradical intermediate were located but their energies relative to that of pyrrole are all significantly higher than experimental activation energies. Alternative pathways for the formation of these products in the closed-shell domain are proposed and investigated. Results of the calculations indicate that *cis*-crotonitrile is likely formed via mechanisms proposed in both the experimental studies and present study. Under high-pressure conditions, the mechanism proposed in the experimental studies may be preferred, but under low-pressure conditions, the mechanism proposed in the present study may be favorable. Allyl cyanide is, on the other hand, more likely formed via the mechanism proposed in the present study. Extensive calculations were carried out to investigate decomposition pathways generating HCN, but we failed to identify a mechanism with a predicted activation energy close to the experimental value of Lifshitz et al. More efforts are needed to understand the details of HCN formation in the pyrolysis of pyrrole.

**Note Added in Proof.** After we submitted this paper for publication, Dubnikova and Lifshitz published a detailed theoretical study of the isomerization mechanism described in Scheme 3 (Dubnikova, F.; Lifshitz, A. *J. Phys. Chem.* **1998**, *102*, 10880–10888). They used the same quantum mechanical methods (uB3LYP for geometry optimization and uQCISD(T) for energy evaluation) but employed a smaller cc-pvdz basis set (number of contracted functions for pyrrole is 95 in cc-pvdz, compared to 100 and 120 in 6-31G(d,p) and 6-311G(d,p) basis sets). Despite the difference in basis sets, their optimized structures are nearly identical to ours. Their relative energies calculated by uB3LYP/cc-pvdz are also very close to ours calculated by uB3LYP/6-31G(d,p), the maximum difference is around 1 kcal/mol. Their relative energies of **TS1** and 2*H*-pyrrole calculated by QCISD(T)/cc-pvdz are also nearly identical to ours calculated by QCISD(T)/6-311G(d,p). However, their relative energies of the open-shell species calculated by uQCISD(T)/cc-pvdz are all significantly lower than our uQCISD(T)/6-311G(d,p) values. For example, their relative energies of **uTS2**, **uE3**, **uTS3**, and **uTS4** reportedly calculated by uQCISD(T)/cc-pvdz without ZPE corrections are 72.42, 69.95, 81.15, and 88.58 kcal/mol, respectively, compared to our corresponding uQCISD(T)/6-311G(d,p) values of 77.3, 71.6, 88.5, and 94.9 kcal/mol. To find out if the difference in basis sets is the origin of the difference in energies, we re-optimized the structures of the open-shell species by uB3LYP/cc-pvdz and recalculated the relative energies by uQCISD(T)/cc-pvdz. Our geometry re-optimization reproduced the structures and uB3LYP/cc-pvdz relative energies of Dubnikova and Lifshitz exactly. The relative energies evaluated by our uQCISD(T)/cc-pvdz calculations at uB3LYP/cc-pvdz structures are 76.0, 69.9, 86.8, and 94.4 kcal/mol. They are very close to our uQCISD(T)/6-311G(d,p) results. Therefore, the difference between our relative energies and theirs is not due to the difference in the basis sets employed in the

two studies. Interestingly, after ZPE correction their uQCISD(T)/cc-pvdz relative energy of **uTS3** (74.0 kcal/mol) is very close to the experimental activation energy of *cis*-crotonitrile formation.<sup>13</sup> Unfortunately, we failed to reproduce their results even though exactly the same methods, structures, and basis set were used.

**Acknowledgment.** We are grateful to one of the reviewers who suggested a closer look for the open-shell biradical intermediate and transition states, which we failed to locate initially. This study was partially supported by the Research and Development Committee of East Tennessee State University and a Cottrel College Science Award of Research Corporation.

## References and Notes

- (1) Snyder, L. R. *Anal. Chem.* **1969**, *41*, 314.
- (2) Attar, A.; Hendrickson, G. G. In *Coal Structure*; Myers, R. A., Ed.; Academic Press: New York, 1985; Chapter 5.
- (3) Pershing, D. W.; Wendt, J. O. *Sixteenth Symposium (International) on Combustion*; The Combustion Institute: Pittsburgh, PA, 1977; p 389.
- (4) Painter, P. C.; Coleman, M. M. *Fuel* **1979**, *58*, 301.
- (5) Turner, D. W.; Andrews, R. L.; Siegmund, C. W. *AIChE Symp. Ser.* **1972**, *68*, No. 126, 55.
- (6) Solomon, P. R.; Colket, M. B. *Fuel* **1978**, *57*, 749.
- (7) Kennedy, L. A. Nitric oxide production from chemically bound nitrogen in fuel-rich coal flames. *Proc. Int. Coal Soc. Conf.* **1981**.
- (8) Dean, A. M.; Hardy, J. E.; Lyon, R. K. Thermal DeNOx. *Nineteenth Symp. (Int.) Combust. [Proc.]* **1982**.
- (9) Perry, R. A.; Steibers, D. L. *Nature* **1986**, *324*, 657.
- (10) Brandenburg, C. F.; Latham, D. R. *J. Chem. Eng. Data* **1968**, *13*, 391.
- (11) Given, P. H. In *Coal Science*; Gorbaty, M. L., Larsen, J. W., Wender, I., Eds.; Academic Press: New York, 1982; Vol. 3, p 65.
- (12) Unsworth, J. F. In *Coal Quality and Combustion Performance*; Unsworth, J. F., Barrat, J. D., Roberts, P. T., Eds.; Elsevier Science Publishers: Amsterdam, 1991; Chapter 4.2, p 206.
- (13) Lifshitz, A.; Tamburu, C.; Suslensky, A. *J. Phys. Chem.* **1989**, *93*, 5802.
- (14) Laskin, A.; Lifshitz, A. *J. Phys. Chem.* **1997**, *101*, 7787.
- (15) Laskin, A.; Lifshitz, A. *J. Phys. Chem.* **1998**, *102*, 928.
- (16) Lifshitz, A.; Bidani, M.; Agranat, A.; Suslensky, A. *J. Phys. Chem.* **1987**, *91*, 6043.
- (17) Mackie, J. C.; Colket, M. B.; Nelson, P. F.; Esler, M. *Int. J. Chem. Kinet.* **1991**, *23*, 733.
- (18) Mackie, J. C.; Colket, M. B.; Nelson, P. F. *J. Phys. Chem.* **1990**, *94*, 4099.
- (19) Zumdahl, S. S. *Chemistry*, 3rd ed.; D. C. Heath and Co.: Lexington, MA, 1993; p 365.
- (20) Grela, M. A.; Amorebieta, V. T.; Colussi, A. J. *J. Phys. Chem.* **1985**, *89*, 38.
- (21) Organ, P. P. Ph.D. Thesis, University of Sydney, 1989.
- (22) Becke, A. D. *J. Chem. Phys.* **1993**, *98*, 5648.
- (23) Lee, C.; Yang, W.; Parr, R. G. *Phys. Rev.* **1988**, *B37*, 785. Miehlich, B.; Savin, A.; Stoll, H.; Preuss, H. *Chem. Phys. Lett.* **1989**, *157*, 200.
- (24) Hehre, W. J.; Ditchfield, R. D.; Pople, J. A. *J. Chem. Phys.* **1972**, *56*, 2257.
- (25) M. J. Frisch, G. W. Trucks, H. B. Schlegel, P. M. W. Gill, B. G. Johnson, M. A. Robb, J. R. Cheeseman, T. Keith, G. A. Petersson, J. A. Montgomery, K. Raghavachari, M. A. Al-Laham, V. G. Zakrzewski, J. V. Ortiz, J. B. Foresman, J. Cioslowski, B. B. Stefanov, A. Nanayakkara, M. Challacombe, C. Y. Peng, P. Y. Ayala, W. Chen, M. W. Wong, J. L. Andres, E. S. Replogle, R. Gomperts, R. L. Martin, D. J. Fox, J. S. Binkley, D. J. Defrees, J. Baker, J. P. Stewart, M. Head-Gordon, C. Gonzalez, and J. A. Pople. *Gaussian 94*, Revision B.1; Gaussian, Inc.: Pittsburgh, PA, 1995.
- (26) Nygaard, L.; Nielsen, J. T.; Kirchheimer, J.; Maltesen, G.; Rastrup-Andersen, J.; Sorensen, G. O. *J. Mol. Struct.* **1969**, *3*, 491.
- (27) Dubnikova, F.; Lifshitz, A. *J. Phys. Chem.* **1998**, *102*, 10880.